

Methyl 2-acetamido-2-deoxy- β -D-glucopyranoside dihydrate and methyl 2-formamido-2-deoxy- β -D-glucopyranoside

Xiaosong Hu, Wenhui Zhang, Allen G. Oliver and Anthony S. Serianni*

University of Notre Dame, Department of Chemistry and Biochemistry,
251 Nieuwland Science Hall, Notre Dame, IN 46556-5670, USA

Correspondence e-mail: aseriann@nd.edu

Received 11 January 2011

Accepted 9 March 2011

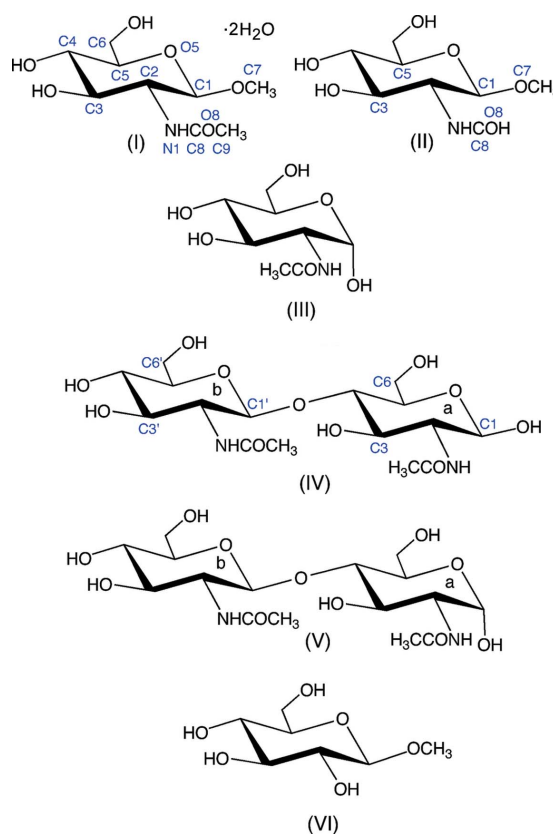
Online 22 March 2011

Methyl 2-acetamido-2-deoxy- β -D-glucopyranoside (β -GlcN-AcOCH₃), (I), crystallizes from water as a dihydrate, C₉H₁₇NO₆·2H₂O, containing two independent molecules [denoted (IA) and (IB)] in the asymmetric unit, whereas the crystal structure of methyl 2-formamido-2-deoxy- β -D-glucopyranoside (β -GlcNFmOCH₃), (II), C₈H₁₅NO₆, also obtained from water, is devoid of solvent water molecules. The two molecules of (I) assume distorted ⁴C₁ chair conformations. Values of φ for (IA) and (IB) indicate ring distortions towards $B_{C2,C5}$ and $C^{3,O5}B$, respectively. By comparison, (II) shows considerably more ring distortion than molecules (IA) and (IB), despite the less bulky *N*-acyl side chain. Distortion towards $B_{C2,C5}$ was observed for (II), similar to the findings for (IA). The amide bond conformation in each of (IA), (IB) and (II) is *trans*, and the conformation about the C–N bond is *anti* (C–H is approximately *anti* to N–H), although the conformation about the latter bond within this group varies by $\sim 16^\circ$. The conformation of the exocyclic hydroxymethyl group was found to be *gt* in each of (IA), (IB) and (II). Comparison of the X-ray structures of (I) and (II) with those of other GlcNAc mono- and disaccharides shows that GlcNAc aldohexopyranosyl rings can be distorted over a wide range of geometries in the solid state.

Comment

Acylation is an important covalent modification that affects the biological functions of saccharides and other biomolecules. Two types of saccharide acylation are common in biological systems, *N*- and *O*-acylation, and recent work has shown that different *O*-acylation patterns affect biological function. For example, this type of covalent control has been described recently for glycopeptidolipids involved in signaling through Toll-like receptors (Sweet *et al.*, 2008). *N*-Acylation is found in biologically relevant monosaccharides, such as *N*-acetyl-D-

glucosamine, *N*-acetyl-D-galactosamine and *N*-acetylneuraminic acid. It has been shown recently that *cis*–*trans* isomerization (CTI) of the amide bond in *N*-acylated sugars can be detected in aqueous solution, with the *cis/trans* ratio dependent on, among other factors, the anomeric configuration of the saccharide (Hu, Zhang *et al.*, 2010). For example, $K_{trans/cis}$ is ~ 60 for methyl *N*-acetyl- α -D-glucosaminide and ~ 38 for methyl *N*-acetyl- β -D-glucosaminide at 326 K. In support of NMR studies of saccharide CTI and of the parameterization of NMR *J* couplings within saccharide exocyclic *N*-acyl fragments (Hu, Carmichael & Serianni, 2010), we undertook the crystallization of methyl 2-acetamido-2-deoxy- β -D-glucopyranoside dihydrate, (I), and methyl 2-formamido-2-deoxy- β -D-glucopyranoside, (II). Their crystal structures, reported here, are compared with the structurally related compounds *N*-acetyl- α -D-glucosamine (2-acetamido-2-deoxy- α -D-glucopyranose), (III) (α -GlcNAcOH; Mo & Jensen, 1975), β -chitobiose [2-acetamido-2-deoxy- β -D-glucopyranosyl-(1 \rightarrow 4)-2-acetamido-2-deoxy- β -D-glucopyranose], (IV) (β -GlcNAcOH and β -GlcNAcOR; Mo, 1979), α -chitobiose [2-acetamido-2-deoxy- β -D-glucopyranosyl-(1 \rightarrow 4)-2-acetamido-2-deoxy- α -D-glucopyranose], (V) (α -GlcNAcOH and β -GlcNAcOR; Mo & Jensen, 1978) and methyl β -D-glucopyranoside, (VI) (β -GlcOCH₃; Jeffrey & Takagi, 1977).



Crystals of (I) and (II) were obtained from aqueous solutions by slow evaporation at room temperature. Compound (I) crystallizes with two independent molecules in the asymmetric unit [denoted (IA) and (IB)] and two solvent water molecules

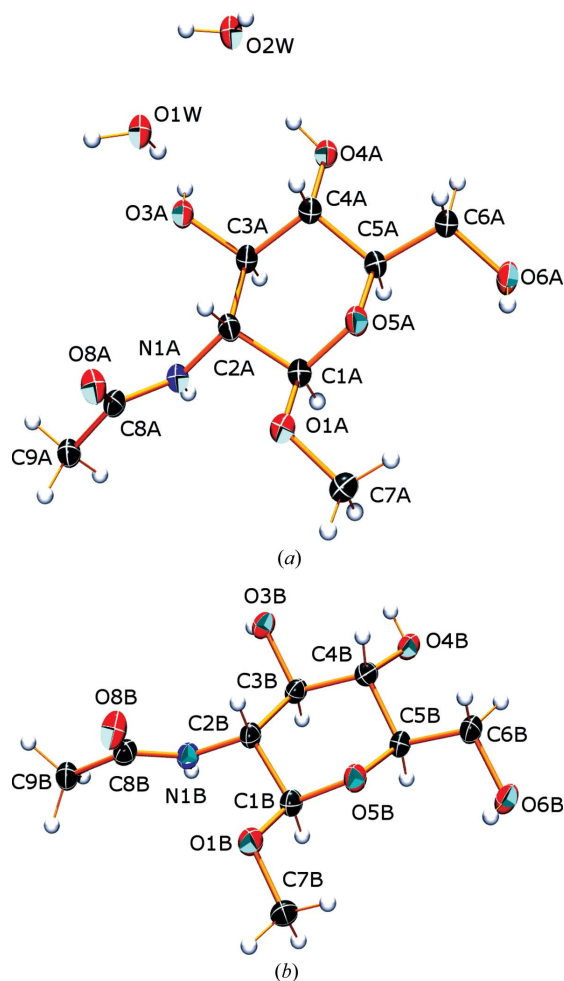


Figure 1
Labeling schemes for (a) molecule (IA) with water molecules and (b) molecule (IB). Displacement ellipsoids are drawn at the 50% probability level.

(Fig. 1a and 1b), whereas the unit cell of (II) contains only one molecule of the saccharide and no solvent water molecules (Fig. 2).

A comparison of selected structural parameters in compounds (I)–(VI) is shown in Table 1. The average C1–C2 and C2–C3 bond lengths in (IA), (IB) and (II) are 1.532 (1) and 1.534 (4) Å, respectively. These values are 0.01–0.02 Å greater than corresponding values in (VI), which are 1.522 (4) and 1.515 (2) Å, respectively, presumably reflecting the different substitutions at C2. All other corresponding C–C bonds in (IA), (IB) and (VI) have very similar lengths. Within the same three structures, the exocyclic C5–C6 bond appears to be the shortest C–C bond [1.516 (3) Å]. Similar inspections of the C1–O1 and C1–O5 bonds suggest a slight lengthening of the former and a slight shortening of the latter in *N*-acyl sugars (IA) and (IB) compared with the related bonds in the simple glycoside (VI).

In all structures in Table 1 bearing an *N*-acyl group, the average C2–N1 bond length is 1.453 (5) Å. This bond is ~0.03 Å longer than the average exocyclic (non-anomeric)

C–OH bond length in a pyranosyl ring, which is 1.427 (4) Å in the same data set.

Within the *N*-acyl exocyclic fragment, the C8–O8 bond averages 1.236 (5) Å, with no discernible difference between *N*-acetyl and *N*-formyl groups. The C8–C9 bond averages 1.502 (8) Å, which is 0.02–0.03 Å shorter than the endocyclic C–C bonds found in the pyranosyl rings.

The *N*-acyl side chains in (IA), (IB) and (II) contain the amide bond N1–C8 in a *trans* conformation, *i.e.* with C2–N1–C8–C9 torsion angles of ± 179.1 (2) $^\circ$ in both (IA) and (IB), and an average C2–N1–C8–O8 torsion angle of 0.77 (2) $^\circ$ in (IA), (IB) and (II). These torsion angles also demonstrate that the amide group is planar. In all three structures, the conformation about the C2–N1 bond is *anti*, *i.e.* atom N1H is roughly *anti* to H2, which is consistent with the behavior reported in solution (Zhu *et al.*, 2006). However, inspection of the C1–C2–N1–C8 and C3–C2–N1–C8 torsion angles in (IA), (IB) and (II) reveals a range of 91–108 $^\circ$ in the former and –128 to –144 $^\circ$ in the latter, indicating some flexibility about the C2–N1 bond in the solid state.

The C5–O5–C1 bond angles in (I)–(VI) appear to depend on anomeric configuration, with β -anomers yielding an average value of 112.0 (6) $^\circ$ and α -anomers an average of 114.7 (3) $^\circ$. Within the full data set, the largest C–C–C bond angle within any given structure (β -anomers only) is C4–C5–C6, which averages 113.8 (11) $^\circ$. The two bond angles that incorporate the carbonyl O atom, O8–C8–C9 and O8–C8–N1, are very similar in each structure and average 122.5 (14) $^\circ$ in the full data set. These results contrast with the remaining angle, N1–C8–C9, which is uniformly smaller than the others in any given structure and averages 116.0 (4) $^\circ$ in the full data set.

Within (IA), (IB) and (II), the endocyclic ring torsion angles vary from 41 to 72 $^\circ$ (absolute values), indicating that aldopyranosyl rings containing *N*-acyl substituents at C2 are distorted. It is noteworthy that the extreme angles within this group are observed in (II), where the C1–C2–C3–C4 and C1–O5–C5–C4 torsion angles are –41.09 (15) and 71.61 (13) $^\circ$, respectively. Within (III)–(VI), these torsion angles range from 48 to 68 $^\circ$ (absolute values). A more quan-

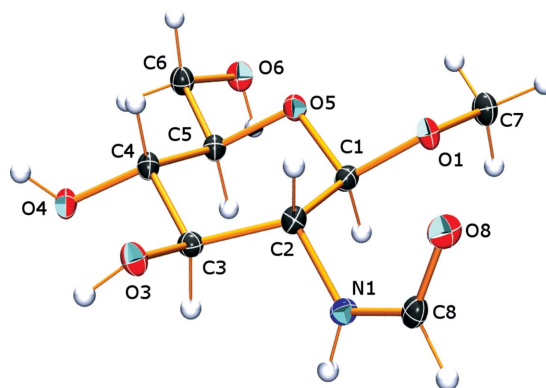


Figure 2
The atom-labeling scheme for compound (II). Displacement ellipsoids are drawn at the 50% probability level.

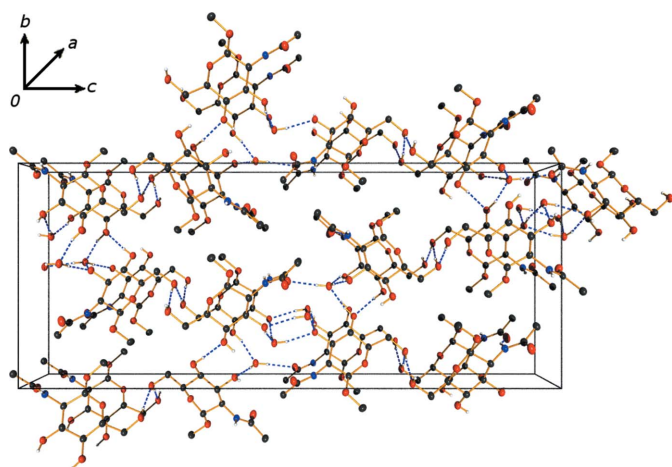


Figure 3
Hydrogen-bonding scheme for molecules (IA) and (IB), viewed along the *a* axis. Dashed lines (blue in the electronic version of the paper) represent hydrogen bonds.

titative treatment of these torsion angles is provided by the Cremer–Pople parameters calculated for (I)–(VI) (Table 2; Cremer & Pople, 1975). The most distorted ring within (I)–(VI) is that of (II), which yields a θ value of 16.59 (14)°. The least distorted ring is found in (Va), where $\theta = 0.9$ (3)°, and the ring is almost an ideal 4C_1 chair. The direction of distortion varies widely within this series of compounds. For (IA) and (II), $\varphi = 302.0$ (12) and 314.4 (5)°, respectively, suggesting distortion towards B_{C_2,C_5} . In contrast, φ for (IB) is 0 (2)°, or a C_3,O_5B distortion. These data show that not only can aldopyranosyl rings be substantially distorted when bearing an *N*-acyl functionality at C2, but the direction of distortion can also vary widely, with various boat (B_{C_2,C_5} , C_3,O_5B and B_{C_1,C_4}) and twist-boat ($C^1TB_{C_5}$, $C^3TB_{C_1}$, $O_5TB_{C_2}$ and $C^5TB_{C_1}$) conformations represented.

The exocyclic hydroxymethyl conformation in each of (IA), (IB) and (II) is *gt* (C4 *anti* to O6), but the *gg* conformation (H5 *anti* to O6) is observed in each of (III), (IVa), (Va) and (Vb). These data show that *gg* and *gt* conformations are favored in GlcNAc/NFm aldopyranosyl rings in the solid state, a behavior which is expected to mimic that in solution, based on related studies of the simpler Glcp anomers (Thibaudeau *et al.*, 2004).

The structure of (I) forms hydrogen-bonded pairs of (IA) and (IB) molecules of through hydroxy atom O6A to atom O6B. In turn, atom O6B forms a hydrogen bond to atom O6Aⁱⁱⁱ of the next pair related by translation along the *a* axis. In addition, the amide groups form hydrogen bonds, although this is to the same GlcNAc molecule related by translation along the *a* axis (all symmetry codes as in Table 3). Amide atom N1A of (IA) has a bifurcated hydrogen bond shared between the adjacent amide carbonyl atom O8Aⁱ and methoxy atom O1Aⁱ. Amide atom N1B of (IB) has a single hydrogen bond to amide atom O8Bⁱ. This association results in chains of pairs of (IA) and (IB) that run through the lattice parallel to the *a* axis. These chains are hydrogen bonded to other chains *via* hydroxy–hydroxy (O4Bⁱ··O4Aⁱⁱ) or hydroxy–water inter-

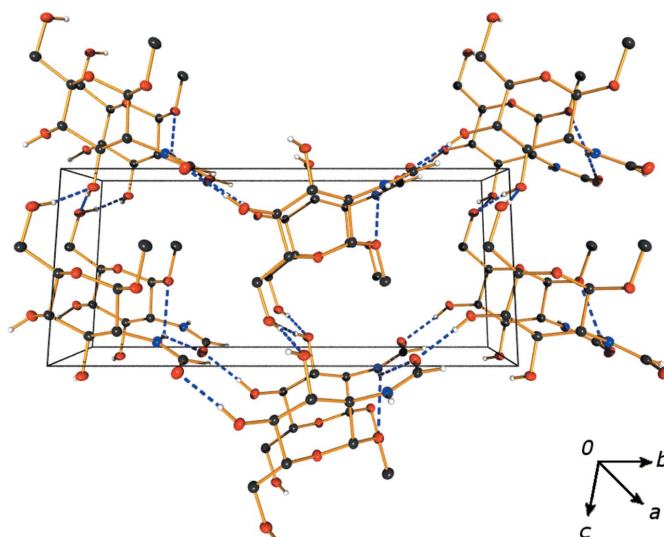


Figure 4
Hydrogen-bonding scheme for (II), viewed along the *a* axis. Dashed lines (blue in the electronic version of the paper) represent hydrogen bonds.

actions. The water molecules are located in a hydrophilic channel lined with amide O atoms (O8B) and hydroxy groups, again parallel to the *a* axis. One motif that is apparent is a hydrogen-bonded ring formed by four sets of these hydrogen-bonded chains. These rings are oriented around a hydrophobic channel formed by the methyl groups of the methoxy moieties and the acetamide methyl group (Fig. 3; see Table 3 for specific details). Overall, this structure forms a highly hydrogen-bonded three-dimensional network of water and amido-saccharide molecules.

The structure of (II) also forms a three-dimensional network of hydrogen-bonded molecules. The network is formed from sheets of (II) that have hydrogen bonds through atom O4 to atom O8ⁱⁱⁱ running parallel to the *b* axis (related by the 2_1 screw axis) and from atom O6 to atom O4^{iv} along the *c* axis, and thus these sheets lie in the *bc* plane of the lattice. Propagation of these sheets into the third dimension is *via* hydrogen bonds from atom O3 to atom O6ⁱⁱ and from atom N1 to atom O8ⁱ of sheets in the next layer along the *a* axis (Fig. 4; all symmetry codes as in Table 4).

Experimental

Compounds (I) and (II) were prepared as described recently in the literature (Hu, Zhang *et al.*, 2010). Both compounds were crystallized from water at room temperature, giving long colorless needle-like crystals that were harvested for X-ray analysis.

Compound (I)

Crystal data

$C_9H_{17}NO_6 \cdot H_2O$	$V = 2356.91$ (8) Å ³
$M_r = 253.25$	$Z = 8$
Orthorhombic, $P2_12_12_1$	Cu $K\alpha$ radiation
$a = 4.6886$ (1) Å	$\mu = 1.06$ mm ⁻¹
$b = 14.4501$ (3) Å	$T = 100$ K
$c = 34.7880$ (7) Å	$0.25 \times 0.03 \times 0.02$ mm

Table 1

Comparison of geometric parameters in compounds (I)–(VI).

gg denotes a *gauche–gauche* conformation and *gt* *gauche–trans*.

Parameter	β -GlcNAc-OCH ₃ (IA)	β -GlcNAc-OCH ₃ (IB)	β -GlcNFM-OCH ₃ (II)	α -GlcNAc-OH (III)	β -GlcNAc-OH (IVa)	β -GlcNAc-OR (IVb)	α -GlcNAc-OH (Va)	β -GlcNAc-OR (Vb)	β -Glc-OCH ₃ (VI)
Bond lengths (Å)									
C1–C2	1.533 (3)	1.531 (3)	1.5318 (19)	1.534 (2)	1.522 (5)	1.522 (3)	1.526 (5)	1.515 (4)	1.522 (4)
C2–C3	1.530 (3)	1.534 (3)	1.5383 (19)	1.531 (3)	1.521 (4)	1.531 (4)	1.527 (5)	1.517 (5)	1.515 (2)
C3–C4	1.527 (3)	1.525 (3)	1.5302 (19)	1.521 (3)	1.531 (3)	1.516 (5)	1.520 (4)	1.516 (4)	1.529 (3)
C4–C5	1.526 (3)	1.523 (3)	1.5284 (18)	1.528 (3)	1.536 (4)	1.507 (5)	1.519 (5)	1.537 (4)	1.527 (4)
C5–C6	1.519 (3)	1.514 (3)	1.5137 (19)	1.514 (2)	1.501 (4)	1.499 (5)	1.512 (5)	1.517 (4)	1.516 (2)
C1–O1	1.389 (3)	1.387 (3)	1.3899 (17)	1.390 (3)	1.389 (4)	1.389 (4)	1.361 (5)	1.395 (4)	1.379 (2)
C1–O5	1.418 (3)	1.423 (3)	1.4198 (17)	1.434 (2)	1.427 (3)	1.429 (3)	1.418 (4)	1.414 (4)	1.433 (2)
C2–N1	1.456 (3)	1.455 (3)	1.4615 (18)	1.457 (2)	1.450 (3)	1.446 (3)	1.450 (4)	1.460 (4)	
C2–O2									1.426 (2)
C3–O3	1.430 (3)	1.424 (3)	1.4282 (16)	1.430 (2)	1.430 (4)	1.424 (4)	1.421 (5)	1.431 (4)	1.425 (4)
C4–O4/O1	1.424 (3)	1.425 (3)	1.4252 (17)	1.434 (2)	1.448 (3)	1.425 (3)	1.448 (3)	1.422 (4)	1.426 (2)
C5–O5	1.443 (3)	1.435 (3)	1.4349 (17)	1.448 (2)	1.429 (3)	1.436 (4)	1.438 (4)	1.427 (5)	1.440 (2)
C6–O6	1.430 (3)	1.430 (3)	1.4341 (17)	1.416 (3)	1.413 (4)	1.415 (5)	1.419 (5)	1.423 (5)	1.417 (4)
C7–O1	1.445 (3)	1.439 (3)	1.4391 (16)						1.430 (4)
C8–O8	1.237 (3)	1.235 (4)	1.2334 (18)	1.235 (2)	1.243 (4)	1.246 (4)	1.231 (4)	1.231 (4)	
C8–C9	1.508 (3)	1.510 (3)		1.508 (3)	1.497 (5)	1.496 (6)	1.490 (6)	1.506 (7)	
Bond angles (°)									
C1–C2–C3	111.22 (19)	109.71 (19)	112.42 (11)	110.11 (13)	111.5 (4)	110.9 (4)	110.0 (2)	109.3 (3)	108.4 (2)
C2–C3–C4	111.5 (2)	111.9 (2)	112.95 (11)	110.88 (15)	109.6 (4)	112.1 (4)	109.7 (3)	109.1 (2)	110.82 (13)
C3–C4–C5	107.7 (2)	110.12 (19)	108.46 (10)	108.77 (15)	111.2 (4)	110.0 (4)	110.7 (3)	110.3 (3)	111.15 (15)
C4–C5–O5	106.79 (19)	108.70 (19)	106.84 (10)	108.41 (13)	110.1 (4)	108.2 (4)	109.3 (2)	110.4 (3)	108.5 (3)
C5–O5–C1	111.9 (2)	111.8 (2)	111.09 (10)	114.97 (14)	112.6 (4)	112.1 (4)	114.5 (3)	112.9 (2)	111.55 (11)
O5–C1–C2	110.80 (19)	108.8 (2)	111.39 (11)	109.24 (15)	109.3 (4)	109.1 (4)	109.6 (3)	110.0 (2)	108.38 (18)
C4–C5–C6	113.9 (2)	112.3 (2)	114.51 (11)	114.77 (16)	113.3 (4)	115.5 (4)	114.3 (3)	113.1 (3)	112.33 (16)
C2–N1–C8	122.6 (2)	121.8 (2)	123.60 (12)	122.17 (18)	122.9 (4)	124.9 (4)	124.8 (3)	122.0 (3)	
N1–C8–C9	116.1 (2)	116.4 (2)		116.01 (18)	116.3 (4)	115.9 (5)	115.3 (3)	115.8 (4)	
O8–C8–C9	121.3 (2)	120.7 (2)		120.93 (16)	122.2 (4)	122.7 (5)	120.7 (3)	120.2 (4)	
O8–C8–N1	122.6 (2)	122.9 (2)	125.18 (13)	123.06 (16)	121.5 (4)	121.3 (4)	123.9 (3)	123.9 (3)	
Torsion angles (°)									
C1–C2–C3–C4	–47.9 (3)	–50.1 (3)	–41.09 (15)	–54.6 (2)	–52.1 (4)	–48.2 (4)	–54.4 (4)	–56.7 (3)	–54.3 (3)
C1–O5–C5–C4	69.3 (2)	66.5 (2)	71.61 (13)	62.5 (2)	61.8 (4)	67.4 (4)	60.4 (3)	59.1 (4)	63.4 (3)
C2–C3–C4–C5	55.1 (3)	50.3 (3)	49.70 (15)	56.8 (2)	50.4 (4)	50.9 (4)	54.5 (3)	54.2 (4)	51.7 (3)
C2–C1–O5–C5	–61.8 (3)	–66.6 (3)	–62.48 (14)	–59.9 (2)	–62.9 (4)	–64.4 (4)	–60.9 (3)	–62.1 (3)	–67.9 (3)
C2–C1–O1–C7/C4	175.5 (2)	169.5 (2)	170.83 (11)			151.7 (4)		161.5 (2)	169.19 (15)
C3–C4–C5–O5	–63.9 (3)	–56.6 (3)	–63.27 (13)	–58.4 (2)	–54.8 (4)	–58.6 (4)	–55.7 (3)	–54.7 (4)	–54.2 (2)
C3–C2–C1–O5	49.6 (3)	56.6 (3)	45.79 (15)	53.8 (4)	57.6 (4)	53.1 (4)	56.5 (4)	60.0 (3)	61.5 (2)
C3–C4–C5–C6	178.8 (2)	–173.9 (2)	178.36 (13)	–177.51 (17)	–174.4 (4)	–178.1 (4)	–174.5 (3)	–175.6 (3)	–171.9 (2)
O5–C5–C6–O6	64.3 (3)	65.2 (3)	66.48 (14)	–60.71 (18)	–60.6 (4)	58.6 (4)	–74.6 (4)	–65.5 (3)	68.7 (3)
C1–C2–N1–C8	<i>gt</i> 108.2 (3)	<i>gt</i> 100.0 (3)	<i>gt</i> 91.34 (14)	<i>gg</i> 140.89 (17)	<i>gg</i> 100.5 (4)	<i>gt</i> 113.7 (4)	<i>gg</i> 138.7 (3)	<i>gg</i> 100.5 (4)	<i>gt</i>
C3–C2–N1–C8	–128.1 (2)	–137.2 (2)	–144.29 (13)	–96.8 (2)	–135.2 (4)	–122.5 (4)	–98.9 (4)	–137.0 (3)	
C2–N1–C8–C9	179.1 (2)	–179.1 (2)		169.86 (15)	–173.7 (4)	178.4 (5)	–179.6 (4)	–173.9 (4)	
C2–N1–C8–O8	<i>trans</i> –1.2 (4)	<i>trans</i> 0.8 (4)	2.7 (2)	<i>trans</i> –9.7 (2)	<i>trans</i> 5.2 (7)	<i>trans</i> –5.3 (6)	<i>trans</i> –2.1 (6)	<i>trans</i> 2.9 (5)	

Data collection

Bruker APEX diffractometer
Absorption correction: multi-scan
(SADABS; Sheldrick, 2008)
 $T_{\min} = 0.760$, $T_{\max} = 0.977$

Refinement

$R[F^2 > 2\sigma(F^2)] = 0.043$
 $wR(F^2) = 0.111$
 $S = 1.06$
4311 reflections
323 parameters
6 restraints
H atoms treated by a mixture of independent and constrained refinement

21482 measured reflections
4311 independent reflections
3722 reflections with $I > 2\sigma(I)$
 $R_{\text{int}} = 0.054$

$\Delta\rho_{\text{max}} = 0.20 \text{ e } \text{Å}^{-3}$
 $\Delta\rho_{\text{min}} = -0.26 \text{ e } \text{Å}^{-3}$
Absolute structure: the configuration was determined based on the known handedness of the chiral C atoms within the structure
Flack parameter: –0.4 (2); 1726 Friedel pairs

Table 2

Cremer–Pople puckering parameters in compounds (I)–(VI).

Compound	θ (°)	φ (°)	Q (Å)	q_2 (Å)	q_3 (Å)	Conformer†
(IA)	11.4 (3)	302.0 (12)	0.595 (3)	0.118 (3)	0.583 (3)	B_{C_2,C_5}
(IB)	7.1 (2)	0 (2)	0.585 (3)	0.078 (2)	0.580 (3)	C_3,O_5B
(II)	16.59 (14)	314.4 (5)	0.5791 (14)	0.1654 (14)	0.5550 (14)	B_{C_2,C_5}
(III)	3.8 (2)	274 (3)	0.582 (2)	0.031 (2)	0.581 (2)	$C^1TB_{C_5}$
(IVa)	4.8 (3)	19 (4)	0.568 (3)	0.044 (3)	0.566 (3)	$C^3TB_{C_1}$
(IVb)	8.7 (3)	338 (2)	0.577 (3)	0.089 (9)	0.570 (3)	$O_5TB_{C_2}$
(Va)	0.9 (3)	55 (3)	0.572 (3)	0.006 (3)	0.572 (3)	B_{C_1,C_4}
(Vb)	2.3 (3)	97 (6)	0.580 (3)	0.029 (3)	0.580 (3)	$C^3TB_{C_1}$
(VI)	6.94 (19)	38 (2)	0.597 (2)	0.072 (2)	0.593 (2)	$C^3TB_{C_1}$

† *B* denotes a boat conformation and *TB* a skew or twist-boat.

Compound (II)

Crystal data

C₈H₁₅NO₆ V = 489.40 (9) Å³
 M_r = 221.21 Z = 2
 Monoclinic, P2₁ Cu Kα radiation
 a = 4.5374 (5) Å μ = 1.11 mm⁻¹
 b = 15.8837 (16) Å T = 100 K
 c = 6.8993 (7) Å 0.34 × 0.07 × 0.06 mm
 β = 100.185 (4)°

Data collection

Bruker APEX diffractometer 6422 measured reflections
 Absorption correction: multi-scan 1744 independent reflections
 (SADABS; Sheldrick, 2008) 1744 reflections with I > 2σ(I)
 T_{min} = 0.703, T_{max} = 0.940 R_{int} = 0.021

Refinement

R[F² > 2σ(F²)] = 0.027 Δρ_{min} = -0.21 e Å⁻³
 wR(F²) = 0.070 Absolute structure: the configura-
 S = 1.06 tion was determined based on the
 1744 reflections known handedness of the chiral C
 137 parameters atoms within the structure.
 1 restraint Flack parameter: 0.13 (14); 806
 H-atom parameters constrained Friedel pairs
 Δρ_{max} = 0.16 e Å⁻³

Table 3

Hydrogen-bond geometry (Å, °) for (I).

D—H...A	D—H	H...A	D...A	D—H...A
O3A—H3OA...O1W ⁱ	0.84	1.85	2.672 (3)	166
O4A—H4OA...O2W	0.84	2.01	2.806 (3)	158
O6A—H6OA...O6B	0.84	2.01	2.837 (3)	170
N1A—H1NA...O8A ⁱ	0.88	2.50	3.132 (3)	129
O3B—H3OB...O2W ⁱⁱ	0.84	1.85	2.658 (3)	160
O4B—H4OB...O4A ⁱⁱ	0.84	2.07	2.898 (2)	167
O6B—H6OB...O6A ⁱⁱⁱ	0.84	1.98	2.815 (3)	173
N1B—H1NB...O8B ⁱ	0.88	2.02	2.838 (3)	154
O1W—H1WA...O3A	0.84 (1)	2.02 (1)	2.843 (3)	167 (3)
O1W—H1WB...O3A ^{iv}	0.84 (1)	2.03 (1)	2.847 (2)	165 (3)
O2W—H2WA...O8A ^v	0.84 (1)	2.01 (1)	2.837 (2)	171 (3)
O2W—H2WB...O3B ^{vi}	0.83 (1)	1.90 (1)	2.728 (3)	174 (3)

Symmetry codes: (i) x - 1, y, z; (ii) -x, y + ½, -z + ½; (iii) x + 1, y, z; (iv) x + ½, -y + ½, -z; (v) x - ½, -y + ½, -z; (vi) -x + 1, y - ½, -z + ½.

The absolute configurations of (I) and (II) were determined both from the known configuration of the starting materials and by comparison of the intensities of Friedel pairs of reflections. However, the Flack parameters were inconclusive [x = -0.4 (2) for (I) and 0.13 (14) for (II); Flack, 1983]. Further confirmation of the configurations was sought by the Hooft analysis, yielding a Hooft y parameter of -0.13 (12) and P2(true) and P3(true) values of 1.000 and 1.000 for (I), and a Hooft y parameter of 0.16 (4) and P2(true) and P3(true) values of 1.000 and 1.000 for (II) (Hooft *et al.*, 2008).

For both structures, the hydroxy, amide and, where applicable, water H atoms were all located from a difference Fourier map and initially included in those positions. The hydroxy and amide H atoms

Table 4

Hydrogen-bond geometry (Å, °) for (II).

D—H...A	D—H	H...A	D...A	D—H...A
N1—H1...O8 ⁱ	0.88	2.29	3.0213 (16)	141
N1—H1...O1 ⁱ	0.88	2.48	3.1621 (15)	134
O3—H3...O6 ⁱⁱ	0.84	1.89	2.7271 (14)	173
O4—H4...O8 ⁱⁱⁱ	0.84	1.90	2.7438 (14)	177
O6—H6...O3 ^{iv}	0.84	1.94	2.7749 (14)	171

Symmetry codes: (i) x - 1, y, z; (ii) x - 1, y, z - 1; (iii) -x, y - ½, -z; (iv) x, y, z + 1.

were subsequently constrained to have reasonable geometric X—H bond distances and angles (N—H = 0.88 Å and O—H = 0.84 Å). Where applicable, mild restraints were applied to the water O—H bond distances [0.84 (1) Å]. All C—H bonds were constrained to distances of 0.98–1.00 Å. For all H atoms, U_{iso}(H) = 1.5U_{eq}(C) for methyl H atoms or 1.2U_{eq}(C) for all others.

Data collection: APEX2 (Bruker–Nonius, 2009) for (I); APEX2 (Bruker–Nonius, 2008) for (II). Cell refinement: SAINT (Bruker–Nonius, 2009) for (I); SAINT (Bruker–Nonius, 2008) for (II). Data reduction: SAINT (Bruker–Nonius, 2009) for (I); SAINT (Bruker–Nonius, 2008) for (II). For both compounds, program(s) used to solve structure: SHELXS97 (Sheldrick, 2008); program(s) used to refine structure: SHELXL97 (Sheldrick, 2008); molecular graphics: XP (Sheldrick, 2008) and POV-Ray (Cason, 2003); software used to prepare material for publication: XCIF (Sheldrick, 2008) and publCIF (Westrip, 2010).

Supplementary data for this paper are available from the IUCr electronic archives (Reference: FA3249). Services for accessing these data are described at the back of the journal.

References

Bruker–Nonius (2008). APEX2 (Version 2008-6) and SAINT (Version 7.53A). Bruker–Nonius AXS Inc., Madison, Wisconsin, USA.
 Bruker–Nonius (2009). APEX2 (Version 2009-9) and SAINT (Version 7.60A). Bruker–Nonius AXS Inc., Madison, Wisconsin, USA.
 Cason, C. J. (2003). POV-Ray. Version 3.6.2. Persistence of Vision Raytracer Pty. Ltd, Victoria, Australia.
 Cremer, D. & Pople, J. A. (1975). *J. Am. Chem. Soc.* **97**, 1354–1358.
 Flack, H. D. (1983). *Acta Cryst.* **A39**, 876–881.
 Hooft, R. W. W., Straver, L. H. & Spek, A. L. (2008). *J. Appl. Cryst.* **41**, 96–103.
 Hu, X., Carmichael, I. & Serianni, A. S. (2010). *J. Org. Chem.* **75**, 4899–4910.
 Hu, X., Zhang, W., Carmichael, I. & Serianni, A. S. (2010). *J. Am. Chem. Soc.* **132**, 4641–4652.
 Jeffrey, G. A. & Takagi, S. (1977). *Acta Cryst.* **B33**, 738–742.
 Mo, F. (1979). *Acta Chem. Scand. Ser. A*, **33**, 207–218.
 Mo, F. & Jensen, L. H. (1975). *Acta Cryst.* **B31**, 2867–2873.
 Mo, F. & Jensen, L. H. (1978). *Acta Cryst.* **B34**, 1562–1569.
 Sheldrick, G. M. (2008). *Acta Cryst.* **A64**, 112–122.
 Sweet, L., Zhang, W., Torres-Fewell, H., Serianni, A. S., Boggess, W. & Schorey, J. (2008). *J. Biol. Chem.* **283**, 33221–33231.
 Thibaudeau, C., Stenutz, R., Hertz, B., Klepach, T., Zhao, S., Wu, Q., Carmichael, I. & Serianni, A. S. (2004). *J. Am. Chem. Soc.* **126**, 15668–15685.
 Westrip, S. P. (2010). *J. Appl. Cryst.* **43**, 920–925.
 Zhu, Y., Pan, Q., Thibaudeau, C., Zhao, S., Carmichael, I. & Serianni, A. S. (2006). *J. Org. Chem.* **71**, 466–479.